Brain Structure and Function (2020) 225:33–43
https://doi.org/10.1007/s00429-019-01980-z

ORIGINAL ARTICLE

FKBP5 methylation predicts functional network architecture of the rostral anterior cingulate cortex

Markus Muehlhan[1,2,3] · Robert Miller[4] · Jens Strehle[3] · Michael N. Smolka[2,5] · Nina Alexander[1]

Received: 18 September 2018 / Accepted: 7 November 2019 / Published online: 14 November 2019

Abstract

DNA methylation (DNA_M) changes in the *FKBP5* gene have been identified as a potential molecular mechanism explaining how environmental adversity may confer long-term health risks. However, the neurobiological correlates of epigenetic signatures in *FKBP5* have only recently been explored in human brain imaging research. The present study aims to investigate associations of *FKBP5* DNA_M and functional network architecture during an implicit emotion regulation task ($N = 74$ healthy individuals). For this, we applied a data-driven multi-voxel pattern analysis (MVPA) to identify regions, where connectivity values vary as a function of *FKBP5* DNA_M, which then served as seed regions for functional network architecture analyses. Blood-derived DNA samples were obtained to analyze quantitative DNA_M at three CpGs sites in intron 7 of the *FKBP5* gene using bisulfite pyrosequencing. MPVA revealed a cluster within the right rostral ACC and the paracingulate ACCs, where connectivity patterns were strongly related to *FKBP5* DNA_M. Using this cluster as seed region for connectivity analyses, we further identified a functional network, including prefrontal, subcortical, insular, and thalamic regions, where connectivity patterns positively correlated with *FKBP5* DNA_M. A subsequent behavioral domain analyses to determine the functional specialization of this network revealed highest effect sizes for subdomains that represent affective and cognitive processes. Together, these findings suggest that *FKBP5* demethylation predicts a widespread functional disruption in a brain network centrally implicated in emotion regulation and cognition, which may in turn convey increased disease susceptibility.

Keywords Epigenetics · Methylation · Functional connectivity · *FKBP5* · FMRI · MVPA · ACC

Introduction

The FK506 binding protein 5 (FKBP5) acts as an important regulator of the hypothalamic–pituitary–adrenal (HPA) axis, the body's major stress response system. Following stress exposure, rising cortisol levels rapidly induce *FKBP5* transcription by activating glucocorticoid response elements (GRE). The protein itself, then provides an ultrashort negative feedback loop for glucocorticoid receptor (GR) signaling via reducing its cortisol-binding affinity and impeding translocation of the receptor complex to the nucleus (Zannas and Binder 2014). Consequently, genetic variants associated with increased *FKBP5* induction, most prominently the rs1360780 T allele, promote GR resistance and impair negative feedback regulation of the HPA axis (Binder et al. 2008). This disruption in regulatory homeostasis ultimately results in chronically elevated glucocorticoid levels, which have been identified as a frequent correlate of stress-related psychopathologies (Chrousos, 2009). Consistent with this notion, the rs1360780 T allele (along with other

Electronic supplementary material The online version of this article (https://doi.org/10.1007/s00429-019-01980-z) contains supplementary material, which is available to authorized users.

✉ Markus Muehlhan
markus.muehlhan@medicalschool-hamburg.de

1 Department of Psychology, Faculty of Human Sciences, Medical School Hamburg, Am Kaiserkai 1, 20457 Hamburg, Germany

2 Neuroimaging Centre, Technische Universität Dresden, Dresden, Germany

3 Department of Psychology, Institute of Clinical Psychology and Psychotherapy, Technische Universität Dresden, Dresden, Germany

4 Department of Psychology, Institute of General Psychology, Biopsychology and Methods of Psychology, Technische Universität Dresden, Dresden, Germany

5 Department of Psychiatry and Psychotherapy, Technische Universität Dresden, Dresden, Germany

high-induction *FKBP5* alleles) is considered a risk factor for stress-related psychiatric disorders (Rao et al. 2016), in particular, upon exposure to environmental adversity (Binder et al. 2008; Wang et al. 2018).

In parallel, genetic neuroimaging studies revealed structural alterations in brain areas involved in emotion processing and regulation of rs1360780 T allele carriers. Specifically, individuals carrying one or two rs1360780 T alleles were found to display larger right amygdala volumes (Hirakawa et al. 2016; Holz et al. 2015), smaller gray matter (GM) volume in the dorsal anterior cingulate cortex (dACC) (Fujii et al. 2014), alterations in hippocampal shape (Fani et al. 2013), and lower white matter (WM) integrity in the left posterior cingulum and the dACC (Fani et al. 2014; Fujii et al. 2014). These findings are complemented by functional magnet resonance imaging (fMRI) experiments demonstrating increased hippocampal and amygdala activity in response to threat (Fani et al. 2013; Holz et al. 2015), as well as altered resting state activity in a frontotemporal–parietal network of rs1360780 T allele carriers (Bryant et al. 2016). In addition, some studies found genotype-related brain changes to further depend on an individual's disease status (Fani et al. 2016; Han et al. 2017; Tozzi et al. 2016) and environmental adversity (Grabe et al. 2016; Holz et al. 2015; White et al. 2012). In a large study comprising 1,826 individuals, reductions in GM volume within three prominent clusters covering the temporal gyrus, the left and hippocampi, the right amygdala, and the anterior cingulate cortices were only observed in those TT carriers with a history of child abuse (Grabe et al. 2016). Likewise, amygdala activity during an emotional face-matching task was found to increase with the severity of emotional neglect in T allele homozygotes (Holz et al. 2015; White et al. 2012). Recent research suggests that such persistent gene-environment (GxE) interactions on neural systems and disease susceptibility might be conferred via epigenetic modifications such as DNA methylation (DNA_M). In a seminal study, childhood trauma has been linked to allele-specific decreases in DNA_M of a GR response element (GRE) located in intron 7 of the *FKBP5* gene, but only in those carrying the rs1360780 T allele (Klengel et al. 2013). This demethylation enhances the transcriptional response of FKBP5 to cortisol, leading to sustained GR resistance and a disruption of the HPA-axis feedback control (Klengel et al. 2013).

Only few studies so far have investigated neural correlates of *FKBP5* DNA_M in brain regions implicated in emotion processing and regulation. Regarding structural integrity, *FKBP5* demethylation has been associated with increased hippocampal volume (Klengel et al. 2013), lower GM volume in the inferior frontal orbital gyrus (Tozzi et al. 2017), and reduced thickness of the right transverse frontopolar gyrus in C allele homozygotes (Han et al. 2017). Moreover, a recent fMRI study reported tentative evidence for a mediating role of *FKBP5* DNA_M status in the association of early life stress and inhibition-related prefrontal activity (Harms et al. 2017). Building on these first studies, an important next step is to identify links between *FKBP5* DNA_M and functional brain network alterations, which often better account for behavioral variance than regional measures of activation (Vaidya and Gordon, 2013). Therefore, this study aims to investigate associations of *FKBP5* DNA_M in intron 7 with functional network architecture during an implicit emotion regulation task. Given that neural correlates of (epi-) genetic variation in *FKBP5* reported in previous studies are not restricted to specific brain regions, we first applied a data-driven multi-voxel pattern analysis (MVPA) to identify regions, where connectivity values vary as a function of DNA_M, which then served as seed regions for subsequent functional network architecture analyses. Based on previous findings, we hypothesized that *FKBP5* demethylation relates to disruptions in clinically relevant brain networks implicated in emotion processing and regulation.

Methods

Sample and procedure

Seventy-four healthy Caucasians participated in the study (male: $n = 45$, age: 23.56 ± 2.36, female: $n = 29$, age 23.17 ± 3.0). All participants were right handed and had normal or corrected to normal vision. Exclusion criteria were current or past mental and/or chronic physical diseases (e.g., asthma, diabetes), medication intake (e.g., psychotropic drugs), pregnancy, and failure to meet MRI compatibility. After a structured telephonic interview, participants were invited for a screening in-person appointment, which consisted of the diagnostic interview for psychiatric disorders–short version (Mini-DIPS) to assess point and lifetime prevalence of axis I disorders on the basis of DSM IV (Margraf 1994) and an in-house checklist on chronic physical diseases, and medication to confirm eligibility. Furthermore, blood samples were drawn into EDTA tubes (Sarstedt, Nümbrecht, Germany) for DNA extraction and stored at − 20 °C for no more than 6 months. For the scanning session, participants were scheduled for a second appointment between 11:00 am and 5:00 pm at the Neuroimaging Centre Dresden and were instructed to arrive well-rested. All participants were carefully introduced to the study protocol and filled in a consent form prior to testing. The scanning session started with the acquisition of structural images to acclimate participants to the scanning environment and to minimize stress reactions related to the scanner setting itself (Muehlhan et al. 2011, 2013). After the structural scan, all participants completed a resting state (RS) measurement followed by an emotional face processing task to assess implicit emotion

regulation. The study was conducted in accordance with the Declaration of Helsinki and approved by the ethics committee of the Technische Universität Dresden [EK: 152052012]. All participants received a monetary compensation of € 30 for participation.

Implicit emotion regulation task

Participants viewed 12 blocks of emotional face stimuli (Fig. 1), each consisting of neutral, fearful, sad, and happy faces taken from the Karolinska Directed Emotional Faces set (Lundqvist et al. 1998), which were presented in a pseudo-randomized order. Each 16-s block consisted of two stimuli per type of facial expressions (with an equal numbers of male and female faces), followed by a 16-s resting period. Stimuli appeared only once and were presented for 800 ms separated by a 300 ms inter-trial-interval. Participants were instructed to discriminate the sex of each face by button-press as fast as possible. The entire task lasted for 6 min and 12 s. The paradigm was programmed using Presentation® (Version 11.3, Neurobehavioral Systems, Inc., Berkeley, CA, USA, www.neurobs.com). Stimuli were presented on an MRI-compatible monitor and viewed via a back-projection mirror. Behavioral responses were acquired using an MRI-compatible response Box (LUMItouchTM, Photon Control Inc. Burnaby, BC, Canada).

Bisulfite pyrosequencing

Quantitative DNA_M analysis of the *FKBP5* gene was performed by Varionostic GmbH (Ulm, Germany). The targeted region contained three CpGs sites corresponding to intron 7 bin 2 in Klengel et al. (2013) that are located within, or in proximity to, a functional consensus GRE (Fig. 2). After extensive screening of functionally relevant regions of the *FKBP5* gene, a seminal study reported that DNA_M levels at these particular sites were found to vary as a function of early trauma, and thus constitutes a promising target for investigating epigenetic correlates of emotion processing and regulation (Klengel et al. 2013). A detailed description of the well-established bisulfite pyrosequencing protocol with amplicon and sequencing primers has been published elsewhere (e.g., Klengel et al. 2013). Briefly, genomic DNA extracted from EDTA whole blood was bisulfite-treated using the EZ DNA Methylation Gold Kit (Zymo Research, Range, CA, USA). Subsequent pyrosequencing was performed on the Q24/ID System, including three human methylation standards (0%, 50%, 100%). Percent DNA_M at each CpG site was quantified using the PyroMark Q24 software

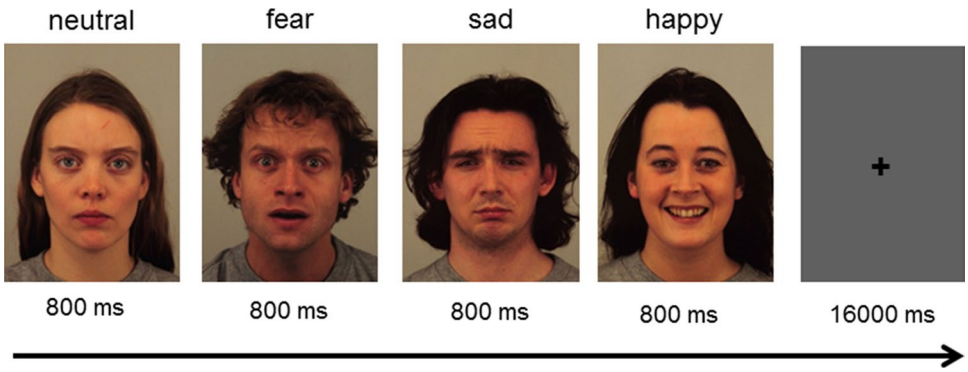

Fig. 1 Schematic illustration of the implicit emotion regulation task depicting an exemplary picture for each facial expression and the consecutive baseline condition

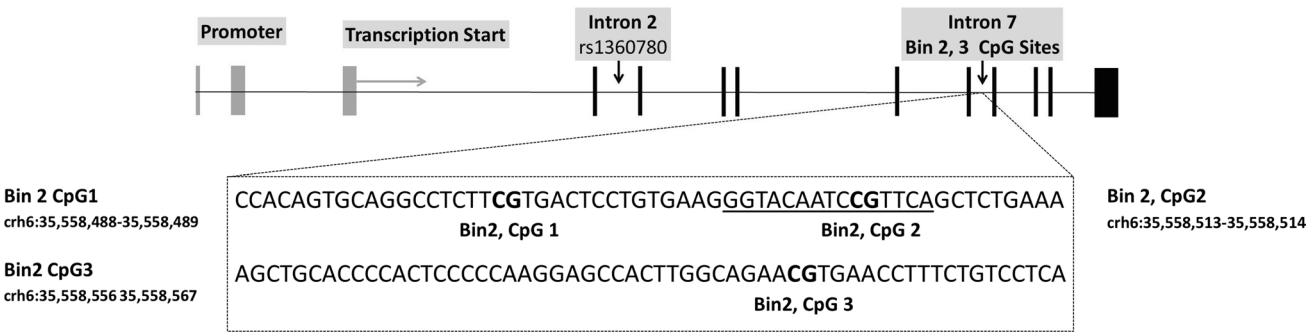

Fig. 2 Schematic representation of the human *FKBP5* gene. The upper panel depicts the *FKBP5* locus in 5′–3′ orientation. Black bars indicate the 11 exons. The lower panel shows the targeted region analyzed by bisulfite pyrosequencing (intron 7 bin 2, comprising three CpG sites marked in bold letters). The functional consensus glucocorticoid response element (GRE) is underlined

(Qiagen) with standard quality control settings implemented in the software. All samples passed quality control. For subsequent analyses, mean percent DNA_M levels across the three CpG sites analyzed within *FKBP5* intron 7 bin 2 were calculated and logit-transformed to achieve normal distribution requirements for statistical testing. Mean *FKBP5* DNA_M levels were 83.95 ± 3.90. Additional analyses revealed that DNA_M patterns were unrelated to sex, age, smoking status, and the use of oral contraceptives in the female subsample (all p values ≥ 0.40). Consequently, these variables were not considered as covariates in subsequent analyses.

FKBP5 rs1360780 genotyping

To rule out potential confounding effects of rs1360780, all participants were genotyped by means of MALDI-TOF mass spectrometry using the MassARRAY-4 system, Complete iPLEX Gold Genotyping Reagent Set, and the GenoTYPER software (Agena Bioscience). The rs1360780 genotype frequencies in our sample are as follows: CC = 45, CT = 21, TT = 8, indicating a slight departure from Hardy–Weinberg equilibrium (HWE: $Chi^2 = 4.38$, $df = 1$, $p = 0.036$). Although deviation from HWE was marginal (i.e. genotype frequencies would be in HWE, if the sample included only one CT instead of one CC carrier); we additionally genotyped rs1360780 by real-time PCR using a LightCycler 480 System (Roche Diagnostics, Mannheim, Germany) to exclude the possibility of genotyping errors. Primers and hybridization probes were customized produced (TIB MOLBIOL, Berlin, Germany). Respective real-time PCR results, 100% replicated the MassARRAY findings. Carriers of the protective rs1360780 genotype (CC) did not differ from risk allele carriers (CT, TT), regarding mean *FKBP5* DNA_M levels ($t = 0.18$, $p = 0.87$).

MRI data acquisition

MRI images were acquired using a 3-Tesla Trio-Tim MRI whole-body scanner (Siemens, Erlangen, Germany). A standard 12-channel head coil and standard headphones were applied. Structural images were obtained using a magnetization prepared rapid gradient echo imaging (MPRAGE) sequence (TR 1900 ms, TE 2.26 ms, flip angle $\alpha = 9°$). Functional measurements were obtained using a T2* weighted gradient echo planar imaging (EPI) sequence (repetition time (TR) 2000 ms, echo time (TE) 25 ms, flip angle $\alpha = 80°$). In each functional run, 179 whole brain volumes of 35 axial slices with a voxel size of 3.4 mm × 3.4 mm × 2.5 mm (25% gap) were acquired sequentially in an ascending order. Each slice had a matrix size of 64 × 64 voxels resulting in a field of view of 220 mm.

fMRI data preprocessing

All analysis steps were performed using the CONN-toolbox v17f (Whitfield-Gabrieli and Nieto-Castanon 2012) running in Matlab R2012a (The MathWorks Inc., Natick, MA, USA). Prior to preprocessing, the first four scans were discharged due to T1 equilibration effects. The remaining 175 scans were spatially realigned and unwarped to correct for interscan movement. Acquisition times were corrected, the structural and functional images were segmented, and all images were directly normalized to the MNI (Montreal Neurological Institute, Quebec, Canada) reference brain. Finally, the functional scans were spatially smoothed using an 8 mm Gaussian kernel. These steps were implemented in the CONN-toolbox as default preprocessing pipeline and based on SPM12 (Wellcome Department of Imaging Neuroscience, UCL, London, UK). Additionally, data artifacts related to movements larger than 0.9 mm to the previous frame or changes in global mean intensity greater than five standard deviations from the mean image intensity for the entire scan were detected using the Artifact Detection Tools (http://www.nitrc.org/projects/artifact_detect).

Two regressors were modeled, which represent the 12 task and 10 resting blocks. Prior to first-level analyses, a denoising procedure including the component-based correction method (CompCor; (Behzadi et al. 2007) and temporal high-pass filtering (> 0.01 Hz) was applied to remove motion, physiological, and other artifactual effects from the fMRI signal. Moreover, the six movement parameters and a matrix containing the ART-detected outliers were included as first-level nuisance covariates.

Multi-voxel pattern analysis (MVPA)

We used the MVPA as implemented in the Conn-toolbox v17.f, which has been used in several prior studies (Thompson et al. 2016; Whitfield-Gabrieli et al. 2016). First, we calculated the pairwise task-related connectivity pattern between each voxel and all other voxels of the brain. The dimensionality of the multi-voxel pattern was reduced using a principle component analysis. For this, 14 components were used which correspond to 20% of the study sample (Hair et al. 2006). Furthermore, a multivariate pattern analysis was performed to calculate associations between any of the 14 components and *FKBP5* DNA_M. This analysis revealed one cluster, located within the right rostral anterior cingulate (rACC) cortex (see results section). In a next step, post hoc analyses were performed using the cluster identified in the MVPA analysis as seed region for seed-to-voxel connectivity analysis to test for associations with *FKBP5* DNA_M. All analyses were conducted using a height threshold of $p < 0.001$; cluster-level family-wise error (FWE) was corrected $p < 0.05$ using a two-sided contrast. Finally,

average functional time series was extracted from each cluster (seed region) and every individual to calculate region of interest-to-region of interest (ROI-to-ROI) connectivity values for a visual inspection of the cluster of points.

Behavioral domain profiling

To characterize the identified brain network in more details, a behavioral domain analysis based on the BrainMap database (brainmap.org) was performed. The BrainMap database contains over 16000 functional imaging experiments classified into five main domains (action, cognition, emotion, interoception, and perception) and 51 subdomains (Fox et al. 2005). These metadata can be used to analyze brain regions with regard to mental processes in which they are involved. The analysis was conducted on April 4th, 2018 and was restricted to "normal mapping" studies. In this search context, only brain mapping studies were considered that have investigated functional activation in healthy subjects. No intervention studies or studies reporting group comparisons were considered. In detail, respective clusters from the seed-to-voxel connectivity analysis were stored as binary masks and transformed into the Talairach space using the software Mango (http://ric.uthscsa.edu/mango/). Afterward, the Behavioral Analysis Plugin (v.: 2.2) was used to check which portion of the coordinates in the BrainMap database is allocated to the masks and whether this differs significantly from a random distribution. This test was repeated for all 51 subdomains and the results were converted to an effect size (z value) corrected for the size of the masks and multiple testing of the 51 subdomains. Only z-values above 3 survived this correction are thus, reported in the results section (Lancaster et al. 2012).

Behavioral data

Reaction time (RT) means and accuracy rates were calculated for each participant. RTs below 100 ms and above 1100 ms were counted as errors and were not considered for further analyses. Subsequent correlation analyses were performed to test for associations between behavioral data (RT and accuracy rates) and seed-to-voxel connectivity, as well as *FKBP5* DNA_M. One person was excluded from the behavioral analyses due to technical problems.

Results

Correlations of functional network architecture and FKBP5 DNA_M: multi-voxel pattern analysis

We first applied a data-driven MVPA to identify potential seed regions for subsequent functional network architecture analyses. The MVPA analysis revealed one cluster where connectivity values varied with *FKBP5* DNA_M (Fig. 3). This cluster has an extension of 111 voxels and comprises parts of the right paracingulate gyrus (paCiG) and the right rACC. The peak voxel of the cluster was located at the MNI coordinates $x = 08$, $y = 48$, $z = -04$. Results are reported at a statistical threshold of $p \leq 0.001$, family-wise error corrected (FWE) at cluster level of $p \leq 0.05$.

Correlations of functional network architecture and FKBP5 DNA_M: seed-to-voxel analysis

Subsequent seed-to-voxel analysis using the MVPA cluster as seed region revealed five clusters, where connectivity values were positively correlated with *FKBP5* DNA_M. For a detailed description of cluster sizes and peak voxels, see Table 1. Seed-to-voxel connectivity maps are depicted in Fig. 4a.

A first cluster within the right hemisphere (peak voxel: $x = 32$, $y = 04$, $z = 02$) covers 26% of the insular cortex (352 voxel), 30% of the putamen (244 voxel), 63% of the frontal operculum (196 voxel), 5% of the temporal pole (130 voxel), 14% of the inferior frontal gyrus pars opercularis (99 voxel), 6% of the central operculum (53 voxel), 3% of the frontal orbital cortex (48 voxel), 15% of the superior temporal gyrus, anterior division (48 voxel), 7% of the inferior frontal gyrus, pars triangularis (41 voxel), 14% of the pallidum (39 voxel), 6% of the planum porale (23 voxel), 1% of the thalamus (13 voxel), and 2% of the caudate (nine voxel). 463 voxel could not be labeled. The second cluster within the left hemisphere (peak voxel:

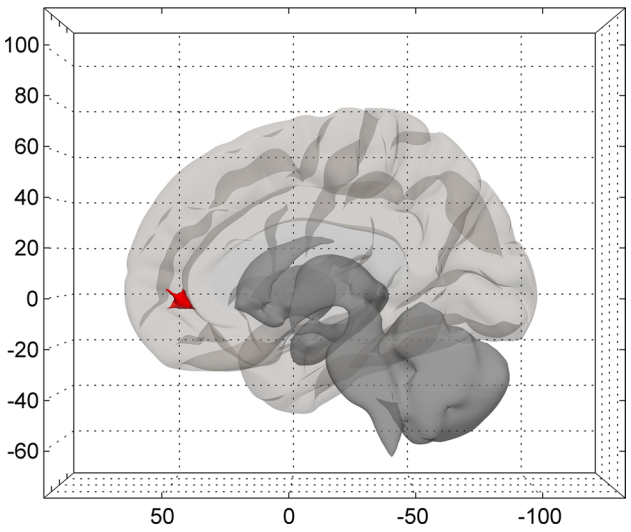

Fig. 3 Results from the multi-voxel pattern analysis (MVPA) are depicted on a right medial view of a gray matter glass brain. Within this rostral ACC cluster, *FKBP5* DNA methylation correlates with connectivity patterns of the MVPA components

Table 1 Peak voxels and cluster sizes derived from correlation analyses of the rostral ACC seed-to-voxel connectivity and *FKBP5* methylation

Region		Hemisphere	Cluster size	MNI coordinates			*Z* value	*β* value
				X	*Y*	*Z*		
1	Putamen	R	1752	32	04	02	4.97	0.55
	Insula	R		40	16	00	4.69	
	Temp. Pol.	R		56	14	− 06	4.62	
2	Putamen	L	777	− 24	10	− 06	4.65	0.50
	Caudate	L		− 20	12	12	4.39	
	Putamen	L		− 28	08	02	4.26	
3	MFG	R	271	42	36	24	4.15	0.41
	MFG	R		34	40	18	3.73	
	IFG	R		40	34	12	3.55	
4	Thalamus	R	160	06	− 16	12	4.42	0.34
5	MFG	L	142	− 32	48	20	4.02	0.33
	MFG	L		− 42	42	16	3.65	

Peak voxels are labeled according to the WFU Pickatlas. Results are reported using a statistical threshold of $p < 0.001$, FWE cluster level corrected ($p < 0.05$) for multiple comparisons. *β* values represent changes in Fisher-*Z*-scores (*z* transformed correlation coefficients) for each unit change in *FKBP5* methylation

IFG inferior frontal gyrus, *MFG* middle frontal gyrus, *Temp. Pol* temporal pole, *β* statistical strength

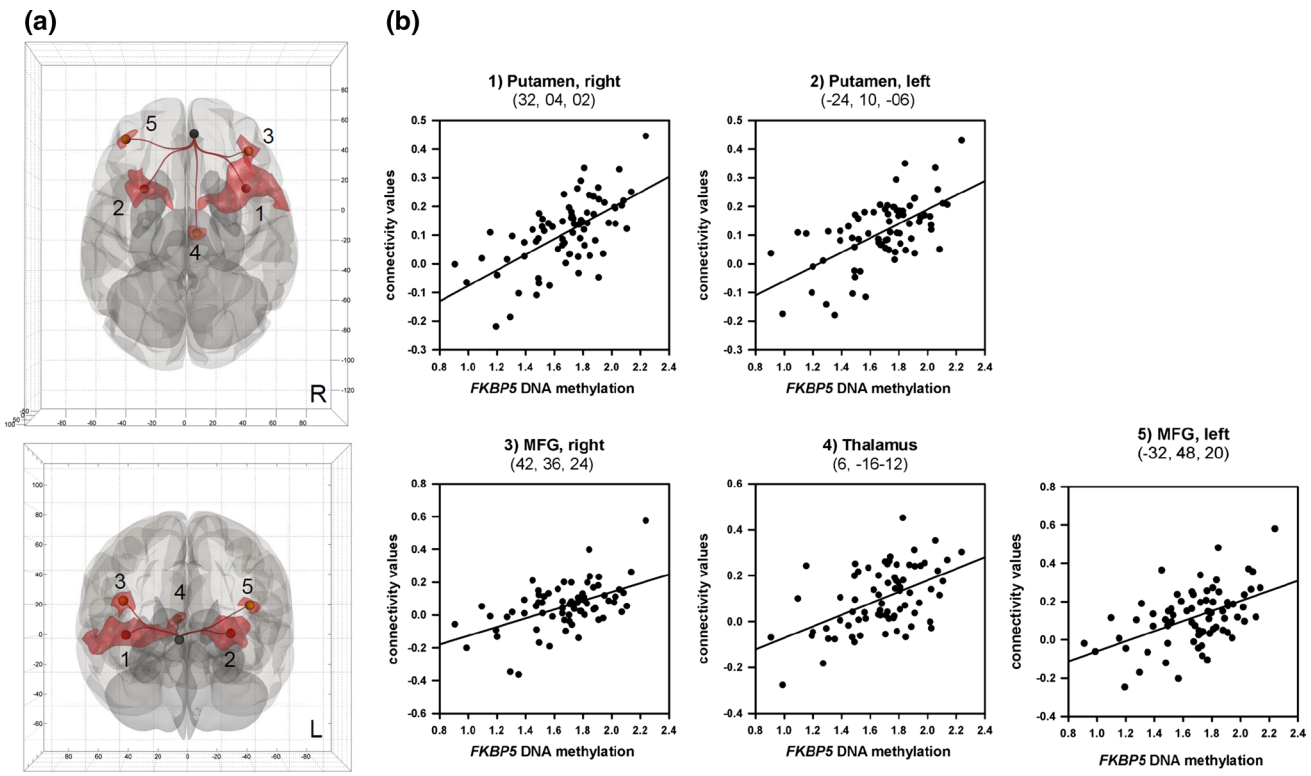

Fig. 4 Results from the subsequent correlational analysis between seed-to-voxel connectivity and *FKBP5* DNA methylation. **a** The seed region was the rostral ACC cluster (black sphere) isolated in the MVPA. The clusters indicate regions were seed-to-voxel connectivity most strongly vary with *FKBP5* DNA methylation. The two-sided contrast is presented using a height threshold of $p < 0.001$, FWE cluster level corrected for multiple comparisons $p < 0.05$. Clusters are depicted on superior and anterior view of a gray matter glass brain. The spheres illustrate the locations of the peak voxel, the red blobs the indicate cluster extensions. **b** Scatterplots for visual inspection illustrate results from subsequent extracted mean connectivity values (ROI-to-ROI analyses) and *FKBP5* methylation. *MFG* middle frontal gyrus. The clusters are labeled according to the location of their peak voxels. A detailed description of the covered brain regions is reported in the text

$x = -24$, $y = 10$, $z = -06$) covers 26% of the putamen (226 voxel), 13% of the insular cortex (174 clusters), 15% of the frontal operculum (53 voxel), 8% of the caudate (41 voxel), 1% of the frontal orbital cortex (21 voxel), 1% of the thalamus (ten voxel), 3% of the pallidum (nine voxel), and 1% of the central opercular cortex (six voxel). 237 voxel could not be labeled. The third cluster (peak voxel: $x = 42$, $y = 36$, $z = 24$) in the right hemisphere covers 2% of the frontal pole (136 voxel), 2% of the middle frontal gyrus (64 voxel), 1% of the inferior frontal gyrus, pars triangularis (five voxel), and 1% inferior frontal gyrus, pars opercularis (four voxel). 62 voxel could not be labeled. The fourth cluster (peak voxel: $x = 06$, $y = -16$, $z = 12$) covers 11% of the right thalamus (140 voxel). Twenty voxel could not be labeled. The fifth cluster (peak voxel: $x = -32$, $y = 48$, $z = 20$) covers 2% of the left frontal pole (135 voxel). Seven voxel could not be labeled. No negative associations between seed-to-voxel connectivity values and *FKBP5* DNA_M could be observed.

For descriptive purposes, we further conducted ROI-to-ROI analyses to calculate the mean connectivity values between the MVPA-based seed region and each of the five clusters from the seed-to-voxel analysis to visualize the positive correlation between connectivity values and *FKBP5* DNA_M (Fig. 4b). Visual inspection of the scatterplots confirmed that the strong positive correlations between *FKBP5* DNA_M and functional connectivity values are not driven by outliers.

The observed associations of *FKBP5* DNA_M with brain connectivity measures were comparable, when controlling for rs1360780 genotype, age and sex in respective analyses. Results are shown in Supplementary Table S1; Figure S2.

Behavioral domain analyses

Histograms of the behavioral domains associated with those clusters where connectivity values varied as a function of *FKBP5* DNA_M were analyzed to determine their functional specialization using behavioral domain metadata extracted from BrainMap. As summarized in Fig. 5, the analysis identified 22 subdomains with the highest effect sizes on the domain "other emotion", which represents general affective processes that do not explicitly fit into other subdomains formulated in the database (see: brainmap.org/taxonomy/behaviors.html#Emotion). Besides further emotion subdomains such as anxiety and disgust, there were also high effect strengths in other subdomains spanning cognition, action, perception, interoception, and language. In addition to the behavioral characterization of the entire network, we further performed behavioral domain analyses for each single cluster (see Figure S 1). These analyses yielded largely comparable results, but revealed that only both clusters covering

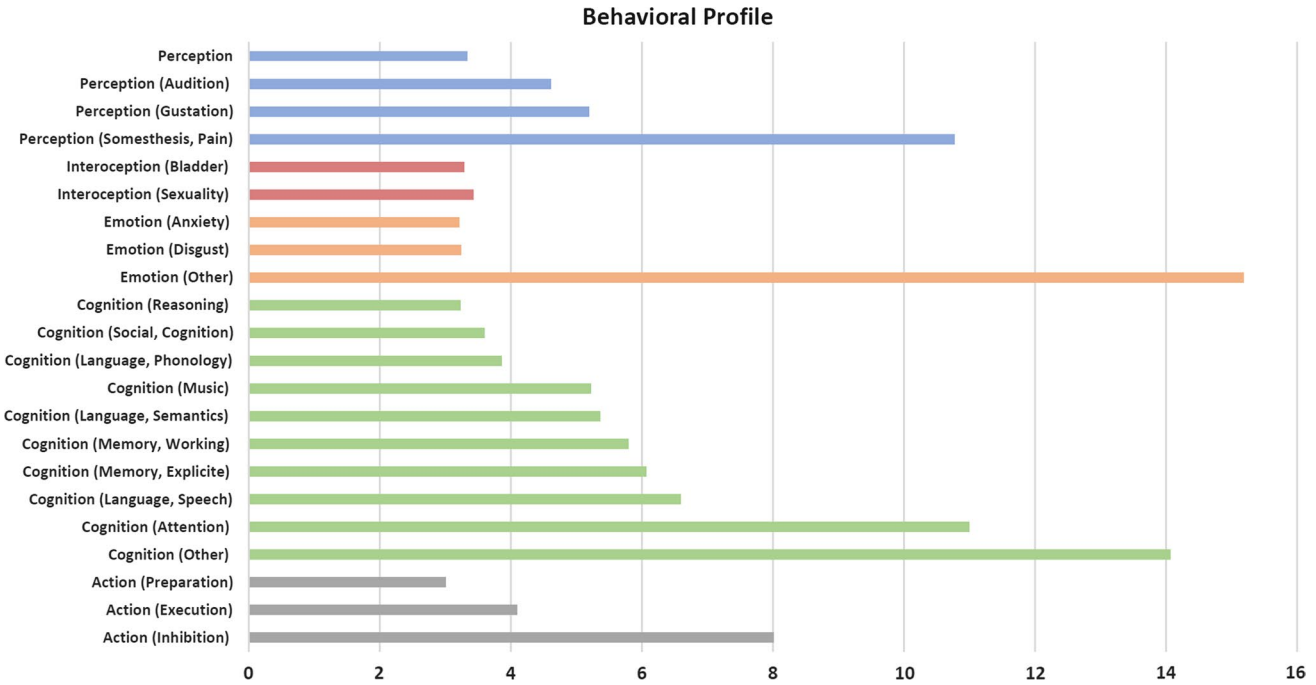

Fig. 5 Behavioral domain analysis. The analysis shows the behavioral profile of the identified ACC-based network associated with *FKBP5* DNA methylation. The results are based on the studies recorded in the brainmap.org database. Only subdomains with an effect size greater than 3 are shown, because these subdomains survived correction for the size of the network mask and for multiple testing across all 51 subdomains

the middle frontal gyri (MFG: cluster 3 and 5) were solely related to the cognitive subdomains working memory and attention.

Behavioral data

Participants showed an average accuracy rate of 94.4% (SD 12.3%) with a mean RT of 571.2 ms (SD 48.5 ms). The correlation analyses between behavioral data with both the ROI-to-ROI connectivity and *FKBP5* DNA_M revealed no significant results.

Discussion

The present study is the first to investigate associations of epigenetic variation in the *FKBP5* gene and functional neural network architecture during an implicit emotion regulation task. Specifically, MVPA revealed a cluster within the right rACC and the adjunct paCiGs, where connectivity patterns were strongly related to *FKBP5* DNA_M. Using this cluster as seed region for subsequent connectivity analyses, we further identified a functional network, including prefrontal, subcortical, insular, and thalamic regions, where connectivity patterns positively correlated with *FKBP5* DNA_M.

These findings significantly extend previous neuroimaging studies investigating neural correlates of genetic variants associated with increased *FKBP5* induction. Specifically, carriers of the high-inducing rs136078 T allele were found to display structural and functional alterations in multiple brain areas involved in emotion regulation that prominently include frontal regions. For example, the rs1360780 T alleles has been linked to smaller GM volume in the dACC (Fujii et al. 2014), lower white matter integrity in the left posterior cingulum, and the dACC (Fani et al. 2014; Fujii et al. 2014), as well as altered resting state activity in a frontotemporal–parietal network (Bryant et al. 2016). In addition, a large MRI study ($N = 1826$ individuals) reported significantly lower GM volumes within three clusters covering the temporal gyrus, the left hippocampi, the right amygdala, and the rACC of child abuse survivors homozygous for the T allele (Grabe et al. 2016). Strikingly, this GxE interaction effect on volume reductions of the rACC corresponds to brain regions that exactly match our MVPA-derived cluster, where functional connectivity patterns were found to vary as a function of *FKBP5* DNA_M. This is interesting in so far as the combination of the T allele and childhood trauma exposure was found to induce a demethylation of *FKBP5* intron 7 bin 2 (Klengel et al. 2013). In turn, this demethylation has been suggested to convey long-term dysregulation of neuroendocrine systems via promoting GR resistance and possibly constitutes a mediating pathway from maltreatment to negative health outcomes (Binder, 2017; Klengel et al. 2013). Our study now suggests that *FKBP5* demethylation relates to impaired functional rACC network architecture, indicating that neural correlates of (epi-) genetic variation linked to enhanced *FKBP5* transcription are not limited to structural rACC changes.

As detailed in comprehensive reviews, the ACC constitutes as a central hub for integrating multimodal information to guide self-regulation and decision making across different domains (Bush et al. 2000; Posner et al. 2007) The rACC (also referred to as pregenual ACC), and adjacent frontal midline structures in specific play a central role in generating emotional responses by coordinating its autonomic, visceromotor, and endocrine components (Kober et al. 2008; Sturm et al. 2013). Among its multiple functions, the rACC is crucially involved in implicit emotion and stress regulation (Etkin et al. 2011; Lederbogen et al. 2011), self-efficacy (Lockwood and Wittmann, 2018), automatic cognitive control (Rive et al. 2013), and further guides the motivation to achieve and maintain task goals (Kober et al. 2008; Wager et al. 2005). A wealth of clinical studies suggests that structural and functional alterations of the rACC range among the most consistently identified neural features of stress-related disorders. For example, significant GM density reductions in the rACC have been reported in patients with PTSD (Bromis et al. 2018) and major depression (Schmaal et al. 2017) compared to healthy controls. These findings are paralleled by fMRI and positron emission tomography (PET) studies demonstrating a general hypoactivation of the rACC in PTSD patients during symptom provocation (Britton et al. 2005; Lanius et al. 2007) and in response to negative or trauma-related stimuli (Shin et al. 2005; Williams et al. 2006). Together, these findings indicate the potential clinical relevance of an aberrant functional rACC connectivity that has been linked to *FKBP5* demethylation in the current study.

With regard to potential mechanisms underlying the association of rACC functional connectivity and *FKBP5* DNA_M, it is important to note that the ACC exhibits a high density of GR (Herman et al. 2005), rendering this area particularly vulnerable to excessive glucocorticoid signaling. It is thus tempting to speculate that *FKBP5* demethylation permanently increases glucocorticoid levels (Klengel et al. 2013), which have been shown to induce neurotoxic effects (Lupien et al. 2018) and functional connectivity changes via dendritic remodeling and effects on postsynaptic dendritic spine plasticity (Hall et al. 2015). With regard to the rACC in specific, circulating cortisol levels and impaired HPA-axis feedback regulation were indeed found to inversely correlate with volume and white matter integrity (fractional anisotropy values) of the rACC (Ota et al. 2013; Treadway et al. 2009). Besides its modulatory effect on the GR, *FKBP5* exerts a broad impact on neuronal functioning and synaptic plasticity, for

example, via regulating mTOR and calcineurin pathways, autophagy, and DNA methyltransferases (Rein, 2016). These findings align well with results from first epigenetic imaging studies that demonstrated associations of *FKBP5* demethylation and impaired morphology in other frontal brain regions (Han et al. 2017; Tozzi et al. 2017). Importantly, our cross-sectional data do not rule out the alternative possibility of pre-existing differences in rACC network architecture as a *cause* for differential *FKBP5* DNA_M. As a central part of the limbic stress regulation system, the rACC significantly modulates the release of GC (Diorio et al. 1993) that have been identified as a crucial mediator of environmentally induced epigenetic changes, including demethylation of the *FKBP5* gene (Klengel et al. 2013). Consequently, longitudinal studies are needed to draw any firm conclusion regarding the causal mechanisms underlying the observed association of epigenetic changes in the *FKBP5* and rACC functional network architecture.

The ACC-based network associated with *FKBP5* DNA_M comprised numerous clusters in prefrontal, subcortical, insular, and thalamic regions. To characterize the functional significance of this network in more detail, we subsequently performed a behavioral domain analysis. As expected for an emotion regulation task, this analysis revealed the overall highest effect strength for emotion subdomains, thus confirming that previous studies have equally highlighted the relevance of the respective network for emotion regulation and processing. Specifically, these emotion subdomains were related to three of the five clusters (referred to as 1, 2, 4 in Table 1), where rACC connectivity values were positively correlated with *FKBP5* DNA_M. These clusters cover relevant brain areas of the basal ganglia structures, including the putamina and the striatum, as well as the insulae, opercula, and thalami. Respective regions are centrally implicated in emotion recognition, the detection of relevant stimuli, salience mapping, motivational processes, and the coordination of different brain networks (Lichev et al. 2015). Besides subdomains related to emotion, behavioral domain analysis identified numerous cognitive subdomains, including working memory, attention, action inhibition, and execution. The involvement of brain regions related to respective cognitive processes appears plausible, given that participants had to keep the task requirement in mind and were instructed to identify the sex of each face by button-press. In addition, higher order cognitive functions and their respective networks have also been suggested to play a decisive role for emotion regulation (LeDoux and Pine, 2016). Lastly, the ACC-based network associated with *FKBP5* DNA_M further consisted of a number of subdomains that appear rather unrelated to the specific task used such as interoception (sexuality, bladder function), perception (perception of pain and taste), music recognition, and language. Some of these domains may offer an interesting starting point for future studies investigating epigenetic underpinnings of maladaptive emotion regulation. For example, a recent meta-analysis concludes that neuronal structures underlying language functions also play a central role in emotion regulation and excessive worrying (Weber-Goericke and Muehlhan, 2018).

Limitations

Several limitations of the present study should be acknowledged. First, reported results rely on peripheral measures of *FKBP5* DNA_M, which may not necessarily generalize to neural tissue. However, post-mortem (Tylee et al. 2013) and studies on living humans (Braun et al. 2017) revealed substantial correlations of DNA_M profiles in peripheral and neural cells, providing a solid base for analyzing DNA_M in blood and saliva samples. Moreover, rodent models revealed parallel changes of *FKBP5* DNA_M profiles in both peripheral cells and neural tissue after chronic corticosterone exposure (Ewald et al. 2014), indicating that DNA_M changes in response to environmental signals appear to be system-wide. Second, we observed no significant correlations of ROI-to-ROI connectivity values and accuracy rates or response times during the implicit emotion regulation task. However, as the experiment consisted of a simple sex discrimination task, it was not designed to produce significant variance in behavioral responses. Finally, findings from the current study remain preliminary until independent replication in larger samples is available.

Conclusion

In conclusion, the present study suggests that *FKBP5* demethylation predicts reduced ACC-based network connectivity with brain areas crucially involved in emotion regulation and cognition. One could speculate that such a poorer recruitment of ACC-based network components might confer deficits in implicit emotional sensitivity and automatic "moment-to-moment" emotion regulation (McRae et al. 2008). These deficits may further affect the transition from implicit to explicit regulation strategies, e.g., when confronted with events of emotional or motivational significance (Gyurak et al. 2011). In addition, an impaired ACC-network connectivity might contribute to an incorrect salience allocation, and thus to poorer explicit emotion regulation strategies. Such impairments in salience mapping and emotion regulation are discussed as a potent risk factor for affective disorders (Etkin et al. 2015; Menon, 2011) that have been previously linked to enhanced *FKBP5* transcription (Wang et al. 2018).

Acknowledgements Funding: This research was supported by the intramural research funding of the TU-Dresden to N.A. and M.M.

M.M. R.M. and M.N.S acknowledged support by the German Research Foundation (Deutsche Forschungsgemeinschaft - DFG) grants CRC (SFB) 940/1 and/or CRC (SFB) 940/2.

We would like to thank Matthis Wankerl and Janin Keitel for assisting in participant recruitment. We further thank Prof. Martin Reuter for carrying out the rs1360780 genotyping in his lab.

Compliance with ethical standards

Ethical statement All procedures performed in studies involving human participants were in accordance with the ethical standards of the institutional and/or national research committee and with the 1964 Helsinki Declaration and its later amendments or comparable ethical standards. The study was approved by the ethics committee of the Technische Universität Dresden [EK: 152052012]. All participants were carefully introduced to the study protocol and filled in a consent form prior to testing.

Conflict of interest The authors have nothing to disclose.

References

Behzadi Y, Restom K, Liau J, Liu TT (2007) A component based noise correction method (CompCor) for BOLD and perfusion based fMRI. NeuroImage 37(1):90–101

Binder EB (2017) Dissecting the molecular mechanisms of gene x environment interactions: implications for diagnosis and treatment of stress-related psychiatric disorders. Eur J Psychotraumatol 8(sup5):1412745

Binder EB, Bradley RG, Liu W, Epstein MP, Deveau TC, Mercer KB et al (2008) Association of FKBP5 polymorphisms and childhood abuse with risk of posttraumatic stress disorder symptoms in adults. JAMA 299(11):1291–1305

Braun P, Hafner M, Nagahama Y, Hing B, McKane M, Grossbach A et al (2017) Genome-wide DNA methylation comparison between live human brain and peripheral tissues within individuals. Eur Neuropsychopharmacol 27:S506

Britton JC, Phan KL, Taylor SF, Fig LM, Liberzon I (2005) Corticolimbic blood flow in posttraumatic stress disorder during script-driven imagery. Biol Psychiat 57(8):832–840

Bromis K, Calem M, Reinders A, Williams SCR, Kempton MJ (2018) Meta-analysis of 89 structural MRI studies in posttraumatic stress disorder and comparison with major depressive disorder. Am J Psychiatry 175:989–998

Bryant RA, Felmingham KL, Liddell B, Das P, Malhi GS (2016) Association of FKBP5 polymorphisms and resting-state activity in a frontotemporal-parietal network. Transl Psychiatry 6(10):e925

Bush G, Luu P, Posner MI (2000) Cognitive and emotional influences in anterior cingulate cortex. Trends Cognit Sci 4(6):215–222

Chrousos GP (2009) Stress and disorders of the stress system. Nat Rev Endocrinol 5(7):374–381

Diorio D, Viau V, Meaney MJ (1993) The role of the medial prefrontal cortex (cingulate gyrus) in the regulation of hypothalamic-pituitary-adrenal responses to stress. J Neurosci 13(9):3839–3847

Etkin A, Egner T, Kalisch R (2011) Emotional processing in anterior cingulate and medial prefrontal cortex. Trends Cognit Sci 15(2):85–93

Etkin A, Buchel C, Gross JJ (2015) The neural bases of emotion regulation. Nat Rev Neurosci 16(11):693–700

Ewald ER, Wand GS, Seifuddin F, Yang X, Tamashiro KL, Potash JB et al (2014) Alterations in DNA methylation of Fkbp5 as a determinant of blood-brain correlation of glucocorticoid exposure. Psychoneuroendocrinology 44:112–122

Fani N, Gutman D, Tone EB, Almli L, Mercer KB, Davis J et al (2013) FKBP5 and attention bias for threat: associations with hippocampal function and shape. JAMA Psychiatry 70(4):392–400

Fani N, King TZ, Reiser E, Binder EB, Jovanovic T, Bradley B et al (2014) FKBP5 genotype and structural integrity of the posterior cingulum. Neuropsychopharmacol 39(5):1206–1213

Fani N, King TZ, Shin J, Srivastava A, Brewster RC, Jovanovic T et al (2016) Structural and functional connectivity in posttraumatic stress disorder: associations with FKBP5. Depress Anxiety 33(4):300–307

Fox PT, Laird AR, Fox SP, Fox PM, Uecker AM, Crank M et al (2005) BrainMap taxonomy of experimental design: description and evaluation. Hum Brain Mapp 25(1):185–198

Fujii T, Ota M, Hori H, Hattori K, Teraishi T, Sasayama D et al (2014) Association between the common functional FKBP5 variant (rs1360780) and brain structure in a non-clinical population. J Psychiatr Res 58:96–101

Grabe HJ, Wittfeld K, Van der Auwera S, Janowitz D, Hegenscheid K, Habes M et al (2016) Effect of the interaction between childhood abuse and rs1360780 of the FKBP5 gene on gray matter volume in a general population sample. Hum Brain Mapp 37(4):1602–1613

Gyurak A, Gross JJ, Etkin A (2011) Explicit and implicit emotion regulation: a dual-process framework. Cognit Emot 25(3):400–412

Hair JFBW, Babin BJ, Anderson RE, Tatham RL (2006) Multivariate data analysis, 6th edn. Pearson Prentice Hall, Upper Saddle River

Hall BS, Moda RN, Liston C (2015) Glucocorticoid mechanisms of functional connectivity changes in stress-related neuropsychiatric disorders. Neurobiol Stress 1:174–183

Han KM, Won E, Sim Y, Kang J, Han C, Kim YK et al (2017) Influence of FKBP5 polymorphism and DNA methylation on structural changes of the brain in major depressive disorder. Sci Rep 7:42621

Harms MB, Birn R, Provencal N, Wiechmann T, Binder EB, Giakas SW et al (2017) Early life stress, FK506 binding protein 5 gene (FKBP5) methylation, and inhibition-related prefrontal function: a prospective longitudinal study. Dev Psychopathol 29(5):1895–1903

Herman JP, Ostrander MM, Mueller NK, Figueiredo H (2005) Limbic system mechanisms of stress regulation: hypothalamo-pituitary-adrenocortical axis. Prog Neuropsychopharmacol Biol Psychiatry 29(8):1201–1213

Hirakawa H, Akiyoshi J, Muronaga M, Tanaka Y, Ishitobi Y, Inoue A et al (2016) FKBP5 is associated with amygdala volume in the human brain and mood state: a voxel-based morphometry (VBM) study. Int J Psychiatry Clin Pract 20(2):106–115

Holz NE, Buchmann AF, Boecker R, Blomeyer D, Baumeister S, Wolf I et al (2015) Role of FKBP5 in emotion processing: results on amygdala activity, connectivity and volume. Brain Struct Funct 220(3):1355–1368

Klengel T, Mehta D, Anacker C, Rex-Haffner M, Pruessner JC, Pariante CM et al (2013) Allele-specific FKBP5 DNA demethylation mediates gene-childhood trauma interactions. Nat Neurosci 16(1):33–41

Kober H, Barrett LF, Joseph J, Bliss-Moreau E, Lindquist K, Wager TD (2008) Functional grouping and cortical-subcortical interactions in emotion: a meta-analysis of neuroimaging studies. NeuroImage 42(2):998–1031

Lancaster JL, Laird AR, Eickhoff SB, Martinez MJ, Fox PM, Fox PT (2012) Automated regional behavioral analysis for human brain images. Front Neuroinf 6:23

Lanius RA, Frewen PA, Girotti M, Neufeld RW, Stevens TK, Densmore M (2007) Neural correlates of trauma script-imagery in posttraumatic stress disorder with and without comorbid major depression: a functional MRI investigation. Psychiatry Res 155(1):45–56

Lederbogen F, Kirsch P, Haddad L, Streit F, Tost H, Schuch P et al (2011) City living and urban upbringing affect neural social stress processing in humans. Nature 474(7352):498–501

LeDoux JE, Pine DS (2016) Using neuroscience to help understand fear and anxiety: a two-system framework. Am J Psychiatry 173(11):1083–1093

Lichev V, Sacher J, Ihme K, Rosenberg N, Quirin M, Lepsien J et al (2015) Automatic emotion processing as a function of trait emotional awareness: an fMRI study. Soc Cognit Affect Neurosci 10(5):680–689

Lockwood PL, Wittmann MK (2018) Ventral anterior cingulate cortex and social decision-making. Neurosci Biobehav Rev 92:187–191

Lundqvist D, Flykt A, Öhman A (1998) The Karolinska directed emotional faces—KDEF, CD ROM from Department of Clinical Neuroscience

Lupien SJ, Juster RP, Raymond C, Marin MF (2018) The effects of chronic stress on the human brain: from neurotoxicity, to vulnerability, to opportunity. Front Neuroendocrinol 49:91–105

Margraf J (1994) Entstehung und Handhabung des Mini-DIPS. Springer, Berlin

McRae K, Reiman EM, Fort CL, Chen K, Lane RD (2008) Association between trait emotional awareness and dorsal anterior cingulate activity during emotion is arousal-dependent. NeuroImage 41(2):648–655

Menon V (2011) Large-scale brain networks and psychopathology: a unifying triple network model. Trends Cognit Sci 15(10):483–506

Muehlhan M, Lueken U, Wittchen HU, Kirschbaum C (2011) The scanner as a stressor: evidence from subjective and neuroendocrine stress parameters in the time course of a functional magnetic resonance imaging session. Int J Psychophysiol 79(2):118–126

Muehlhan M, Lueken U, Siegert J, Wittchen HU, Smolka MN, Kirschbaum C (2013) Enhanced sympathetic arousal in response to FMRI scanning correlates with task induced activations and deactivations. PLoS One 8(8):e72576

Ota M, Hori H, Sato N, Sasayama D, Hattori K, Teraishi T et al (2013) Hypothalamic-pituitary-adrenal axis hyperactivity and brain differences in healthy women. Neuropsychobiology 68(4):205–211

Posner MI, Rothbart MK, Sheese BE, Tang Y (2007) The anterior cingulate gyrus and the mechanism of self-regulation. Cognit Affect Behav Neurosci 7(4):391–395

Rao S, Yao Y, Ryan J, Li T, Wang D, Zheng C et al (2016) Common variants in FKBP5 gene and major depressive disorder (MDD) susceptibility: a comprehensive meta-analysis. Sci Rep 6:32687

Rein T (2016) FK506 binding protein 51 integrates pathways of adaptation: FKBP51 shapes the reactivity to environmental change. BioEssays 38(9):894–902

Rive MM, van Rooijen G, Veltman DJ, Phillips ML, Schene AH, Ruhe HG (2013) Neural correlates of dysfunctional emotion regulation in major depressive disorder A systematic review of neuroimaging studies. Neurosci Biobehav Rev 37(10 Pt 2):2529–2553

Schmaal L, Hibar DP, Samann PG, Hall GB, Baune BT, Jahanshad N et al (2017) Cortical abnormalities in adults and adolescents with major depression based on brain scans from 20 cohorts worldwide in the ENIGMA Major Depressive Disorder Working Group. Mol Psychiatry 22(6):900–909

Shin LM, Wright CI, Cannistraro PA, Wedig MM, McMullin K, Martis B et al (2005) A functional magnetic resonance imaging study of amygdala and medial prefrontal cortex responses to overtly presented fearful faces in posttraumatic stress disorder. Arch Gen Psychiatry 62(3):273–281

Sturm VE, Sollberger M, Seeley WW, Rankin KP, Ascher EA, Rosen HJ et al (2013) Role of right pregenual anterior cingulate cortex in self-conscious emotional reactivity. Soc Cognit Affect Neurosci 8(4):468–474

Thompson WH, Thelin EP, Lilja A, Bellander BM, Fransson P (2016) Functional resting-state fMRI connectivity correlates with serum levels of the S100B protein in the acute phase of traumatic brain injury. NeuroImage Clin 12:1004–1012

Tozzi L, Carballedo A, Wetterling F, McCarthy H, O'Keane V, Gill M et al (2016) Single-nucleotide polymorphism of the FKBP5 gene and childhood maltreatment as predictors of structural changes in brain areas involved in emotional processing in depression. Neuropsychopharmacology 41(2):487–497

Tozzi L, Farrell C, Booij L, Doolin K, Nemoda Z, Szyf M et al (2017) Epigenetic changes of FKBP5 as a link connecting genetic and environmental risk factors with structural and functional brain changes in major depression. Neuropsychopharmacology 43:1138

Treadway MT, Grant MM, Ding Z, Hollon SD, Gore JC, Shelton RC (2009) Early adverse events, HPA activity and rostral anterior cingulate volume in MDD. PLoS One 4(3):e4887

Tylee DS, Kawaguchi DM, Glatt SJ (2013). On the outside, looking in: a review and evaluation of the comparability of blood and brain "-omes". Am J Med Genet Part B, Neuropsychiatr Genet 162B(7): 595–603

Vaidya CJ, Gordon EM (2013) Phenotypic variability in resting-state functional connectivity: current status. Brain Connect 3(2):99–120

Wager TD, Jonides J, Smith EE, Nichols TE (2005) Toward a taxonomy of attention shifting: individual differences in fMRI during multiple shift types. Cognit Affect Behav Neurosci 5(2):127–143

Wang Q, Shelton RC, Dwivedi Y (2018) Interaction between early-life stress and FKBP5 gene variants in major depressive disorder and post-traumatic stress disorder: a systematic review and meta-analysis. J Affect Disord 225:422–428

Weber-Goericke, F, Muehlhan, M. (2018): A quantitative meta-analysis of fMRI studies investigating emotional processing in excessive worriers: application of activation likelihood estimation analysis. J Affect Disord (epub ahead of print)

White MG, Bogdan R, Fisher PM, Munoz KE, Williamson DE, Hariri AR (2012) FKBP5 and emotional neglect interact to predict individual differences in amygdala reactivity. Genes Brain Behav 11(7):869–878

Whitfield-Gabrieli S, Nieto-Castanon A (2012) Conn: a functional connectivity toolbox for correlated and anticorrelated brain networks. Brain Connect 2(3):125–141

Whitfield-Gabrieli S, Ghosh SS, Nieto-Castanon A, Saygin Z, Doehrmann O, Chai XJ et al (2016) Brain connectomics predict response to treatment in social anxiety disorder. Mol Psychiatry 21(5):680–685

Williams LM, Kemp AH, Felmingham K, Barton M, Olivieri G, Peduto A et al (2006) Trauma modulates amygdala and medial prefrontal responses to consciously attended fear. NeuroImage 29(2):347–357

Zannas AS, Binder EB (2014) Gene-environment interactions at the FKBP5 locus: sensitive periods, mechanisms and pleiotropism. Genes Brain Behav 13(1):25–37